

Theoretical analysis of unambiguous 2-D tracking loop performance for band-limited BOC signals

Yang Gao¹ · Zheng Yao¹  · Mingquan Lu¹

Received: 16 August 2017 / Accepted: 26 December 2017
© Springer-Verlag GmbH Germany, part of Springer Nature 2018

Abstract

Code-tracking accuracy, an important attribute of receiver performance assessment, depends both on characteristics of the ranging signal being tracked and on the structure of the tracking channel. The implementation of binary offset carrier (BOC) modulated signals and the development of new tracking channel structures with a two-dimensional (2-D) loop architecture, in which both the code and subcarrier delays are estimated independently by two separate tracking loops, have resulted in the theories of 2-D loop tracking performance being of increased interest. However, the theories of tracking performance in white noise for band-limited BOC signals using the most representative and most mature 2-D tracking method are still not mature. Therefore, we present the exact expression for tracking performance prediction for limited front-end bandwidths to show how well double estimator technique (DET) could perform for given conditions. While evaluation of the exact expression requires numerical integration, a simple yet accurate closed-form analytical approximation is also provided for a more intuitive description of tracking performance. Moreover, we present a bandwidth-dependent, quasi-optimal, discriminator parameter selection rule to simplify the work of receiver designers while improving tracking performance. These results can provide further guidance for the design, parameters selection, and optimization of the receiver.

Keywords Binary offset carrier · Unambiguous tracking · Tracking accuracy · Two-dimensional · Double estimator · Quasi-optimal parameters selection

Introduction

With better spectrum separation and wider root-mean-square (RMS) bandwidth than legacy signals (Betz 2001), binary offset carrier (BOC) modulated signals (Betz 1999), which adopt a subcarrier to move the main spectrum component away from the carrier frequency, are widely adopted as new ranging signals in the new-generation global navigation satellite systems (GNSS) (Rebeyrol et al. 2007). However, BOC modulation introduces an ambiguity threat into the code-tracking process (Mongredien et al. 2011) due to its multi-peak auto-correlation function (ACF). Side peak lock may occur creating a bias in pseudorange measurements. In order to solve the ambiguity problem, new tracking channel structure with a two-dimensional (2-D) loop architecture in which both the code and subcarrier delays are estimated

independently by two separate tracking loops, have been proposed in recent years. Representative existing methods include the double estimator technique (DET) (Hodgart et al. 2007; Hodgart and Simons 2012) and the double phase estimator (DPE) (Borio 2014a, b). 2-D tracking techniques are more general and have better performance as confirmed by several parties (Anantharamu et al. 2009; Julien et al. 2010; Ruegamer et al. 2011) compared to the one-dimensional (1-D) unambiguous tracking technique for BOC signals in which only one tracking loop is used to track the variation of the delay of the code replica and subcarrier replica (Fine and Wilson 1999; Kao and Juang 2012; Yao et al. 2010). Moreover, 1-D tracking can be regarded as a special case of 2-D tracking as the code delay and subcarrier delay are forced to be the same.

Although 2-D unambiguous tracking techniques for BOC signals have become of increasing interest in recent years, the theories of their tracking performance predictions are still not mature unlike the established theory for predicting the code-tracking accuracy for conventional binary phase shift keying (BPSK) modulated signals (Betz and

✉ Zheng Yao
yaozheng@tsinghua.edu.cn

¹ Department of Electronic Engineering, Tsinghua University, Beijing 100084, China

Kolodziejki 2000, 2009a, b). On the one hand, existing performance analysis methods (Borio 2014b; Hodgart et al. 2007) do not account for the effects of band limiting at the receiver front-end. On the other hand, the traditional code-tracking theory cannot be directly applied to these cases due to the coupling relation between dimensions which cannot be ignored (Hodgart and Simons 2012; Yao et al. 2017). Therefore, existing performance analysis methods cannot accurately reflect the actual performance of the receiver and may even mislead the receiver designer. Accordingly, we focus on the 2-D tracking performance analysis of band-limited BOC signals in consideration of the coupling relation between dimensions and take the most representative 2-D tracking technique DET as an example to show our analysis because it is the most mature technique and has the greatest number of degrees of freedom. The results presented herein are of reference value to other 2-D tracking methods that are related to or are evolved from DET.

First, the exact expression for tracking performance prediction in white noise under a limited front-end bandwidth is presented using DET for unambiguous processing of BOC signals. This analysis will describe how well DET could perform for given conditions thus providing further guidance for receiver designs.

Second, while the exact expression is accurate for tracking performance prediction, it is complicated, it does not provide much intuitive insight, and it requires numerical integration in its evaluation. We also present a simpler, yet still accurate, closed-form analytical approximation, derived from the exact expression. This simplified expression can significantly reduce the computational cost of theoretical tracking performance prediction and can also more clearly and intuitively reveal the influence of key parameters on DET tracking accuracy required for receiver design, such as front-end bandwidth and early–late discriminator spacing. Both the exact expression and the closed-form analytical approximation can help provide guidance for receiver designers.

Third, based on the exact expression and the closed-form approximation, we present a simple yet useful quasi-optimal discriminator parameter selection rule for a given bandwidth using DET in the sense of minimum tracking jitter. The numerical results presented verify the correctness and general applicability of the selection rule. This conclusion can provide strong guidance for the selection and optimization of the receiver key parameters, thus greatly simplifying the designers' work while improving tracking performance.

We first formalize the BOC signal model and DET structure. Then we present the exact theoretical prediction of DET tracking accuracy in band-limited white noise and derive its closed-form analytical approximation. This section also provides the quasi-optimal strategy of DET parameters selecting. A set of numerical results is then provided in a special

section to explore the effects of various key parameters on tracking performance and compare the different expressions and approximations. Finally, conclusions are discussed. The appendix outlines essential steps in deriving the expressions.

Signal and system models

This section formulates a BOC signal model and DET structure. It assumes that the received signal is unaffected by multipath. Therefore, a radio frequency (RF) BOC signal at the antenna of the receiver can be modeled as

$$r(t) = \sqrt{2C}d(t - \tau)g_c(t - \tau)b_{\text{BOC}}(t - \tau)\cos(2\pi f_{\text{RF}}t + \varphi) + n(t) \quad (1)$$

where C is signal power, $d(t)$ is the navigation message, $g_c(t)$ is the bipolar spreading code signal whose value takes ± 1 with spreading code rate f_c , τ is the signal propagation delay, f_{RF} is the RF frequency with the Doppler, φ is the phase of the carrier, $n(t)$ is zero-mean Gaussian white noise with power spectrum density (PSD) N_0 , $b_{\text{BOC}}(t) \triangleq \text{sgn}[\sin(2\pi f_{sc}t)]$ is a sine-phased square wave subcarrier with subcarrier frequency f_{sc} , where $\text{sgn}(x)$ is the sign function which takes the value of 1 for $x \geq 0$ and -1 for $x < 0$. We define $T_c = 1/f_c$ and $T_s = 1/(2f_{sc})$ as the code chip period and subcarrier chip period, respectively, where the latter corresponds to half the wavelength of the subcarrier.

Using the terminology from (Betz 1999), a sine-phased BOC signal can be denoted as $\text{BOC}_{\text{sin}}(p, q)$, where p is the ratio of f_{sc} to GNSS baseline frequency $f_0 = 1.023$ MHz, and q presents the ratio of f_c to f_0 . Note that a cosine-phased BOC signal in which the derivation process and conclusions are similar to the sine-phased BOC case can also be adopted. Therefore, we mainly discuss the sine-phased BOC signals.

The signal (1) is first amplified at the front-end of the receiver and subjected to band-limited filtering, which is then fed into a loop of the DET structure, as shown in Fig. 1. It is assumed that the carrier is ideally removed. Unlike a conventional 1-D code-tracking loop, the code delay τ_c and the subcarrier delay τ_s are estimated by two separate tracking loops, respectively. Receivers generate three local code components which are early (E) replica $g_c(t - \tau_c + \Delta_c/2)$, prompt (P) replica $g_c(t - \tau_c)$ and late (L) replica $g_c(t - \tau_c - \Delta_c/2)$, and three local subcarrier components which are E replica $b_{\text{BOC}}(t - \tau_s + \Delta_s/2)$, P replica $b_{\text{BOC}}(t - \tau_s)$ and L replica $b_{\text{BOC}}(t - \tau_s - \Delta_s/2)$. Δ_c and Δ_s are the spacing between E and L replicas for the code discriminator and the subcarrier discriminator, respectively, and they are assumed to be in the ranges $0 < \Delta_c \leq T_c$ and $0 < \Delta_s \leq T_s$.

The product of the local code and subcarrier is subjected to the coherent integration of length T with the received signal and $T \gg T_c$, resulting in a 2-D cross-correlation function (CCF) which is a bivariate function of τ_c and τ_s . For P

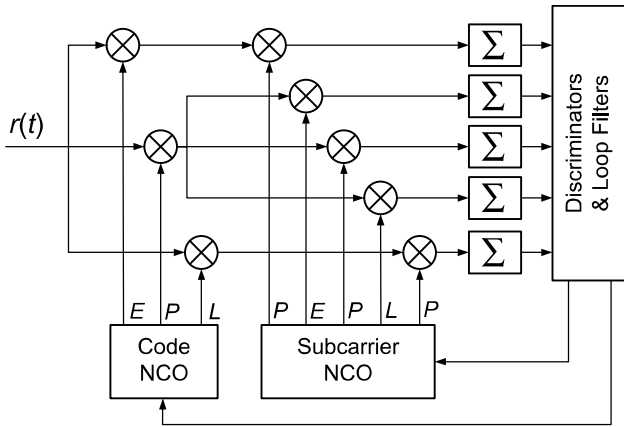


Fig. 1 Structure of double estimator technique

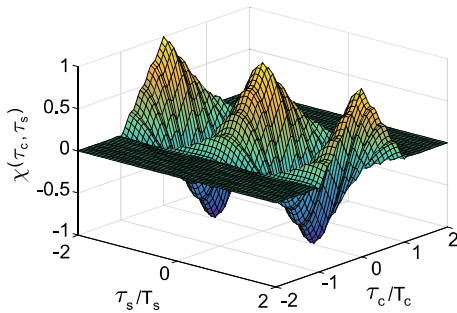


Fig. 2 Band-limiting two-dimensional ACF of $\text{BOC}_{\text{sin}}(2, 1)$ signal, where $\beta_r = 3f_0$

replica, the 2-D CCF in normalized units of amplitude \sqrt{C} can be written as

$$\chi(\tau_c, \tau_s) = \frac{1}{T} \int_0^T [g_c(t - \tau) b_{\text{BOC}}(t - \tau) * h(t)] \cdot g_c(t - \tau_c) b_{\text{BOC}}(t - \tau_s) dt \quad (2)$$

where $*$ indicates convolution, and $h(t)$ is the unit impulse response of the ideal low-pass filter with one-sided bandwidth β_r . For conciseness and without loss of generality, we always assume that $\tau = 0$.

Figure 2 shows the band-limiting 2-D ACF of a $\text{BOC}_{\text{sin}}(2,1)$ signal, where $\beta_r = 3f_0$, which is just large enough to contain two main lobes of the $\text{BOC}_{\text{sin}}(2,1)$ signal spectrum. It can be seen from the figure that $\chi(\tau_c, \tau_s)$ roughly presents a triangular peak in the code dimension and presents a triangular wave with a period T_s in the subcarrier dimension. Therefore, the tracking error from code dimension and from subcarrier dimension can be open-loop estimated with the early–late discriminator

$$\mathbf{e} = \boldsymbol{\delta}(\boldsymbol{\tau}) + \boldsymbol{\varepsilon} \quad (3)$$

where $\mathbf{e} = [e_c, e_s]^T$, e_c and e_s are code dimension and subcarrier dimension discriminator output, respectively, and are used to control feedback loops to continuously track the delays. $\boldsymbol{\tau} = [\tau_c, \tau_s]^T$, $\boldsymbol{\delta}(\boldsymbol{\tau}) = [\delta_c(\tau_c, \tau_s), \delta_s(\tau_c, \tau_s)]^T$, δ_c and δ_s are S-curves of code dimension and subcarrier dimension, respectively, and are denoted as

$$\begin{cases} \delta_c(\tau_c, \tau_s) = \chi(\tau_c - \Delta_c/2, \tau_s) - \chi(\tau_c + \Delta_c/2, \tau_s) \\ \delta_s(\tau_c, \tau_s) = \chi(\tau_c, \tau_s - \Delta_s/2) - \chi(\tau_c, \tau_s + \Delta_s/2) \end{cases} \quad (4)$$

Further, $\boldsymbol{\varepsilon}_c$ and $\boldsymbol{\varepsilon}_s$ are code and subcarrier discrimination noise, respectively, where $\boldsymbol{\varepsilon} = [\varepsilon_c, \varepsilon_s]^T$, whose covariance matrix is \mathbf{N} .

Since $T_s < T_c$, it is not difficult to prove that when the two discriminator outputs of (3) are close to zero, the code loop can provide an unambiguous but noisier delay estimator $\hat{\tau}_c \approx \tau$, and the subcarrier loop can provide a high-accuracy but ambiguous delay estimator $\hat{\tau}_s \approx \tau + NT_s$, where N is an arbitrary integer. Furthermore, an unambiguous and high-accuracy final delay estimator can be obtained by the following formula

$$\hat{\tau} \approx \hat{\tau}_s - \hat{N}T_s \quad (5)$$

where $\hat{N} = \text{round}[(\hat{\tau}_s - \hat{\tau}_c)/T_s]$ is the estimator of N .

Theoretical tracking performance prediction

This section takes full account of the effects of band-limiting and the coupling relation between dimensions, which are ignored by previous studies (Borio 2014b; Hodgart et al. 2007), and describes the DET tracking performance. The

exact expression for tracking performance prediction, the simpler closed-form analytical approximation, and quasi-optimal discriminator parameters selection rule are all presented. As will be shown later in our discussion, ignoring the coupling relation between dimensions may mislead tracking performance analysis.

Exact expression for tracking accuracy

Linearizing (3) around $\boldsymbol{\tau} = [0, 0]^T$ yields

$$\mathbf{e} \approx \mathbf{K}\boldsymbol{\tau} + \boldsymbol{\varepsilon} \quad (6)$$

where

$$\mathbf{K} = \partial \boldsymbol{\delta}(\boldsymbol{\tau}) / \partial \boldsymbol{\tau} |_{\boldsymbol{\tau}=[0,0]^T} \quad (7)$$

is denoted as the slope matrix, whose elements $\partial\delta_i(\tau_c, \tau_s)/\partial\tau_j|_{\tau_c=\tau_s=0}$ for $i, j \in \{c, s\}$ are discriminator slopes which reflect the sensitivity of the discriminator to errors.

The covariance matrix of the open-loop estimations of τ in normalized units of subcarrier chip periods squared can then be obtained by

$$\frac{1}{T_s^2} \mathbf{Q} = \frac{1}{T_s^2} \begin{bmatrix} q_c & q_{cs} \\ q_{sc} & q_s \end{bmatrix} = (T_s \mathbf{K})^{-1} \mathbf{N} \left((T_s \mathbf{K})^{-1} \right)^T \quad (8)$$

If the final delay estimator is calculated through (5), the open-loop delay estimation accuracy is only dependent on the estimation accuracy of τ_s , with variance q_s .

Expanding the matrix operation on the right side of (8), using the relationship between open-loop accuracy and closed-loop accuracy given in (Betz and Kolodziejewski 2009a; Yao et al. 2017), we can obtain the closed-loop delay estimation variance of DET in normalized units of subcarrier chip periods squared, which is

$$\left(\frac{\sigma_\tau}{T_s} \right)^2 = \frac{B_L(1 - 0.5B_LT)}{C/N_0} \cdot \frac{(\kappa_{sc}^2 n_{cc} + \kappa_{cc}^2 n_{ss} - 2\kappa_{sc}\kappa_{cc}n_{cs})}{(\kappa_{cc}\kappa_{ss} - \kappa_{cs}\kappa_{sc})^2} \quad (9)$$

where B_L is the one-sided equivalent loop bandwidth, $\kappa_{ij} = T_s \cdot \partial\delta_i(\tau_c, \tau_s)/\partial\tau_j|_{\tau_c=\tau_s=0}$, and $n_{ij} = 2TN_0^{-1} \mathbb{E}\{\varepsilon_i\varepsilon_j\}$, for $i, j \in \{c, s\}$.

Yao et al. (2017) gives the exact expression of the normalized 2-D ACF (2) of band-limiting BOC signals

$$\begin{aligned} \chi(\tau_c, \tau_s) = & \int_{-\beta_r}^{\beta_r} \eta(f) \{ \cos(2\pi f[\Lambda(\tau_c - \tau_s) - \tau_c]) \\ & - \frac{\text{sgn}(\Lambda(\tau_c - \tau_s))}{\tan(\pi f T_s)} [\sin(2\pi f[\Lambda(\tau_c - \tau_s) - \tau_c]) \\ & + \sin(2\pi f \tau_c)] \} df \end{aligned} \quad (10)$$

where $\eta(f) \triangleq T_c \text{sinc}^2(\pi f T_c) \tan^2(\pi f T_s)$ is the PSD of BOC signal, $\text{sinc}(x) = \sin(x)/x$, and $\Lambda(t) \triangleq t - \lfloor t/(2T_s) \rfloor + 1/2$ is the sawtooth wave of the period $2T_s$. When the early–late code discriminator spacing Δ_c is close to integral multiples of T_s , in which $\Delta_c/2$ can be decomposed into $\Delta_c/2 \approx k_2 \cdot 2T_s + k_1 \cdot T_s + k_0 \cdot T_s/2$ where $k_2 \in \mathbb{N}$ and k_1 and k_0 can only take 0 or 1, then $\Lambda(t)$ and $\text{sgn}(\Lambda(t))$ in (10) can be largely simplified. Under this condition, substituting (10) into (4), then using (7), after algebraic simplification, one can obtain

$$\begin{aligned} \kappa_{sc} &= - \int_{-\beta_r}^{\beta_r} v(f) df \\ \kappa_{ss} &= \int_{-\beta_r}^{\beta_r} v(f) \frac{\cos(\pi f(\Delta_s - T_s))}{\cos(\pi f T_s)} df \end{aligned} \quad (11)$$

where $v(f) \triangleq 4\pi T_s f \eta(f)/\tan(\pi f T_s)$. It can be seen from (11) that κ_{sc} and κ_{ss} are not related to Δ_c . However, κ_{cc} and κ_{cs} are related to Δ_c . When Δ_c is close to an odd multiple of T_s , i.e., $k_0 = 1$, one can obtain

$$\begin{aligned} \kappa_{cc} &= (-1)^{k_1} \int_{-\beta_r}^{\beta_r} v(f) \cos(\pi f \Delta_c) df \\ \kappa_{cs} &= (-1)^{k_1+1} \int_{-\beta_r}^{\beta_r} v(f) \frac{\cos(\pi f \Delta_c)}{\cos(\pi f T_s)} df \end{aligned} \quad (12)$$

Further, when Δ_c is close to an even multiple of T_s , i.e., $k_0 = 0$, one can obtain

$$\begin{aligned} \kappa_{cc} &\approx 0 \\ \kappa_{cs} &= (-1)^{k_1} \int_{-\beta_r}^{\beta_r} v(f) \tan(\pi f T_s) \sin(\pi f \Delta_c) df \end{aligned} \quad (13)$$

The entries of the normalized covariance matrix are

$$\begin{aligned} n_{cc} &= \int_{-\beta_r}^{\beta_r} 4w(f) \sin^4(\pi f \Delta_c/2) df \\ n_{cs} &= n_{sc} = - \int_{-\beta_r}^{\beta_r} w(f) \frac{4 \sin^2(\pi f \Delta_c/2) \sin(\pi f \Delta_s/2) \sin[\pi f(\Delta_s - 2T_s)/2]}{\cos(\pi f T_s)} df \\ n_{ss} &= \int_{-\beta_r}^{\beta_r} w(f) [-1 + \cos(\pi f \Delta_s) + \sin(\pi f \Delta_s) \tan(\pi f T_s)]^2 df \end{aligned} \quad (14)$$

where $w(f) = 4T_c \text{sinc}^2(\pi f T_c)$.

It is worth noting that the non-diagonal elements κ_{sc} and κ_{cs} of the normalized slope matrix are both nonzero, which implies that the tracking errors of the subcarrier dimension and code dimension do have an influence on each other's discriminator output. Therefore, the coupling relation between dimensions cannot be ignored. Otherwise, some important phenomenon cannot be observed. The most typical phenomenon, neglected in previous studies is that the selection of Δ_c significantly affects the final ranging accuracy. Contrasting (12) with (13), it can be noted that $\kappa_{cc} \approx 0$ when Δ_c is close to an even multiple of T_s . This means the code discriminator in this situation will be very insensitive to the delay variation, resulting in a greater code-tracking jitter than that when Δ_c is close to an odd multiple of T_s . Further, greater code-tracking jitter affects the subcarrier loop tracking accuracy due to the coupling relation between dimensions, resulting in a worse final ranging accuracy. Therefore, the tracking accuracy with Δ_c being confined to even multiples of T_s is generally worse than that with Δ_c confined to odd multiples of T_s .

In order to verify this fact, considering BOC_{sin}(2,1) signal as an example, Fig. 3 shows the theoretical prediction results of tracking performance using (9) under different Δ_c , where the one-sided front-end bandwidth is $\beta_r = 3f_0$, the loop bandwidth is $B_L = 1$ Hz, the coherent integration time is $T = 1$ ms, and the subcarrier early–late spacing is

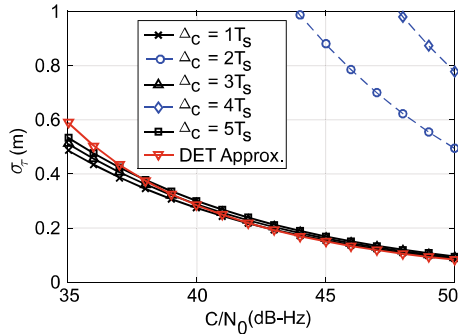


Fig. 3 Tracking jitters of DET with different code early–late spacing $\Delta_c = iT_s$, $i = 1, 2, 3, 4, 5$

$\Delta_s = 0.5T_s$. It can be easily seen from the figure that the selection of Δ_c does have a significant effect on the final ranging performance and Δ_c should be chosen as close as possible to an odd multiple of T_s to achieve better tracking performance. In contrast, the infinite bandwidth approximation curve in the literature (Borio 2014b) is also given in the figure, denoted as DET Approx. However, it cannot reflect the influence of Δ_c on tracking accuracy due to ignoring the effect of coupling relation between dimensions.

In addition to the code early–late spacing Δ_c , it can be seen from (11) to (14) that there are other important receiver parameters which can influence the ranging performance, such as early–late subcarrier discriminator spacing Δ_s and front-end bandwidth β_r . With the help of the exact expression (9), receiver designers can analysis the DET tracking performance under different conditions by using numerical integration. Some specific numerical results will be given in the next section.

Approximate expression for tracking accuracy

As mentioned previously, although the exact expression (9) can accurately describe the DET tracking performance, it is complicated, it does not provide much intuitive insight, and it requires numerical integrations in its evaluation. Therefore, it is not convenient to use the exact expression for analysis of the influence of receiver key parameters, such as front-end bandwidth and early–late discriminator spacing, on the tracking performance. In view of this, we present a simpler yet still accurate closed-form analytical approximation, derived from the exact expression, which can provide intuitive guidance to the receiver designer.

It can be seen from the previous analysis, Δ_c should be chosen as close as possible to an odd multiple of T_s to achieve better tracking performance. Furthermore, Fig. 3 shows that when Δ_c takes on different odd multiples of T_s , the final tracking accuracy changes little. Therefore, the

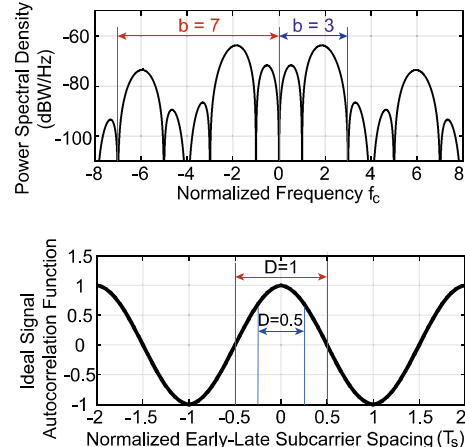


Fig. 4 Definition of normalized one-sided front-end bandwidth b and normalized early–late subcarrier discriminator spacing D . (Top) PSD of $\text{BOC}_{\sin}(2,1)$ signal and two different values of b . (Bottom) Profile of 2-D ACF in τ_s dimension with $\tau_c = 0$ and two different values of D

following analysis takes $\Delta_c = 1T_s$ as an example to analyze the influence of other receiver key parameters on the tracking performance. It should be noted that analysis methods and conclusions proposed below are similar when Δ_c is set to another odd multiple of T_s .

For conciseness, we define the normalized one-sided front-end bandwidth as $b \triangleq \beta_r/f_c$, and the normalized two-sided early–late subcarrier discriminator spacing as $D \triangleq \Delta_s/T_s$. The top and bottom panels in Fig. 4 illustrate the definition of b and D , respectively.

It can be verified by numerical calculation of (11) and (12) that $\kappa_{cc} \approx -\kappa_{sc}$ is always applicable no matter when Δ_c takes any odd multiple of T_s . Based on this fact, the exact expression (9) can be approximated as

$$\left(\frac{\sigma_\tau}{T_s}\right)^2 \approx \frac{B_L(1 - 0.5B_LT)}{C/N_0} \cdot Y \cdot \Gamma \quad (15)$$

where Y and Γ are defined as

$$Y \triangleq \frac{\kappa_{sc}^2 + \kappa_{cc}^2 - \kappa_{sc}\kappa_{cc}}{3 \cdot (\kappa_{cc}\kappa_{ss} - \kappa_{cs}\kappa_{sc})^2} \quad (16)$$

$$\Gamma \triangleq n_{cc} + n_{ss} + 2n_{cs} \quad (17)$$

where Y and Γ are independently determined by the slope matrix and the noise covariance matrix, respectively.

Considering the $\text{BOC}_{\sin}(\alpha k, k)$ signal, assume the normalized one-sided front-end bandwidth b is wide enough to contain two main lobes of the $\text{BOC}_{\sin}(\alpha k, k)$ signal spectrum, i.e., $b \geq \alpha+1$. Using the approximate relationship

$$\text{Si}(x) \approx \Psi(x) = \begin{cases} \pi \text{sgn}(x)/2 & |x| \geq 3\pi/2 \\ -0.28 \cos(x) + \pi/2 & \pi/2 \leq |x| \leq 3\pi/2 \\ x & |x| \leq \pi/2 \end{cases} \quad (18)$$

and

$$F(x) \approx \Phi(x) = \begin{cases} x \text{sgn}(x)\pi/2 & |x| \geq \pi \\ \cos(x) + x \cdot \text{Si}(x) & |x| < \pi \end{cases} \quad (19)$$

where $\text{Si}(x) \triangleq \int_0^x \text{sinc}(t)dt$ is the sine integral function and $F(x) \triangleq \cos(x) + x \cdot \text{Si}(x)$ is the integral of $\text{Si}(x)$, Eq. (15) is approximately simplified as

$$\left(\frac{\sigma_\tau}{T_s}\right)^2 \approx \begin{cases} \frac{B_L(1-0.5B_L T)}{C/N_0} \cdot \left(\frac{\alpha}{4\alpha-1}\right)^2 \cdot \left[\left(4-\frac{2}{\alpha}\right)D + \frac{1}{\alpha}\right] & bD \geq 3\alpha \\ \frac{B_L(1-0.5B_L T)}{C/N_0} \cdot \left(\frac{\alpha\pi}{2(4\alpha-1)(-0.28\cos(\frac{bD}{2\alpha}\pi)+\frac{\pi}{2})}\right)^2 \cdot \left[\left(4-\frac{2}{\alpha}\right)D + \frac{1}{\alpha}\right] & b \geq 3\alpha, \alpha \leq bD < 3\alpha \\ \frac{B_L(1-0.5B_L T)}{C/N_0} \cdot \left(\frac{\alpha^2}{(4\alpha-1)bD}\right)^2 \cdot \left[\frac{2(2\alpha-1)}{\alpha^2}bD^2 + \frac{1}{\alpha}\right] & b \geq 3\alpha, bD < \alpha \\ \frac{B_L(1-0.5B_L T)}{C/N_0} \cdot \frac{\tilde{\kappa}_{cc}^2 + \tilde{\kappa}_{ss}^2 - \tilde{\kappa}_{sc}\tilde{\kappa}_{cs}}{3 \cdot (\tilde{\kappa}_{cc}\tilde{\kappa}_{ss} - \tilde{\kappa}_{cs}\tilde{\kappa}_{sc})^2} \cdot \zeta & \alpha + 1 \leq b < 3\alpha \end{cases} \quad (20)$$

where

$$\begin{aligned} \tilde{\kappa}_{cc} &\approx \frac{1}{\alpha\pi} \cdot 2\text{Si}\left(\frac{b}{2\alpha}\pi\right) \\ \tilde{\kappa}_{cs} &= \tilde{\kappa}_{sc} \approx -\frac{4}{\alpha\pi} \left(\text{Si}\left(\frac{b}{\alpha}\pi\right) - \frac{\pi}{4}\right) \\ \tilde{\kappa}_{ss} &\approx \frac{2}{\alpha\pi} \left[(4\alpha-1)\text{Si}\left(\frac{bD}{2\alpha}\pi\right) + (1-4\alpha)\text{Si}\left(\frac{b(D-2)}{2\alpha}\pi\right) - (4\alpha-3)\text{Si}\left(\frac{b(D+2)}{2\alpha}\pi\right) - \frac{\pi}{2} \right] \end{aligned} \quad (21)$$

and

$$\begin{aligned} \zeta &= \frac{1}{b\pi^2} \left\{ -(8\alpha+2) - (4\alpha-2)\frac{bD}{\alpha}\pi^2 + (4\alpha-1)\frac{b}{\alpha}\pi^2 \right. \\ &\quad \left. + (8\alpha-4)\Phi\left(\frac{bD}{\alpha}\pi\right) + 8\Phi\left(\frac{b(1-D)}{2\alpha}\pi\right) - 8\alpha\Phi\left(\frac{b(1-D)}{\alpha}\pi\right) \right\} \end{aligned} \quad (22)$$

The function waveforms of $\text{Si}(x)$ and its approximation are plotted in Fig. 5 via (18). Specific approximation and simplification processes are provided in Appendix.

It can be seen from (20) that the closed-form analytical approximation with code early–late spacing Δ_c confined to odd multiples of subcarrier chip period T_s , is divided into four different sections due to the relative position of b and D in the $D - b$ plane, which means there are four regions that need to be considered separately in the receiver parameter space. These regions are defined in terms of b and D , which constitute the receiver parameter space. Once the front-end bandwidth b and subcarrier early–late spacing D are given, a closed-form analytical approximation (20) can be used to predict the tracking performance of $\text{BOC}_{\sin}(\alpha k, k)$ signal.

Figure 6 shows a schematic representation of these four different regions in the $D - b$ plane given by closed-form analytical approximation. It should be noted that the front-end bandwidth, which is the horizontal axis in this figure, is normalized in units in order to adapt all the $\text{BOC}_{\sin}(\alpha k, k)$ signals.

The region defined by $bD \geq 3\alpha$ is referred to as spacing dominant, since the predicted tracking error depends primarily on the subcarrier early–late spacing but not the front-end bandwidth. The region defined by $bD < \alpha$ and $b \geq 3\alpha$ is referred to as bandwidth dominant since the subcarrier early–late spacing is restricted to a limited range

$$\begin{aligned} bD \geq 3\alpha & \\ b \geq 3\alpha, \alpha \leq bD < 3\alpha & \\ b \geq 3\alpha, bD < \alpha & \\ \alpha + 1 \leq b < 3\alpha & \end{aligned}$$

and the predicted tracking error is mainly determined by the front-end bandwidth. The condition $\alpha \leq bD < 3\alpha$ and $b \geq 3\alpha$ indicates a transition region between the two distinct dominant cases. The region defined by $b < 3\alpha$ is referred to as the complicated region, since the predicted tracking error is complicated due to the combined effects of band-limiting and coupling relation between dimensions.

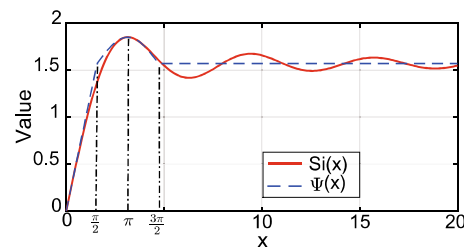


Fig. 5 Function waveforms of $\text{Si}(x)$ and its approximation $\Psi(x)$

Unlike the exact expression (9), the closed-form analytical approximation (20) does not require numerical integration, which not only can significantly reduce the computational cost of theoretical tracking performance prediction, but also can more clearly and intuitively reveal the influence of key parameters of receiver, such as front-end bandwidth β_r and early–late subcarrier discriminator spacing Δ_s , on DET tracking accuracy. Therefore, the closed-form analytical approximation can provide intuitive guidance for the selection and optimization of receiver parameters.

Quasi-optimal parameter selection

For receiver designers, there are two aspects of significant concern. One is how to predict the tracking error under given conditions; the other is how to choose the optimal discriminator spacing for a given bandwidth to minimize the tracking error. The former can be solved by the exact expression (9) and the closed-form analytical approximation (20). The following analysis will focus on the latter, that is, the optimal discriminator parameters selection rule for a given bandwidth, which can be easily obtained by using the simplified yet still accurate closed-form analytical approximation (20).

When $b \geq 3\alpha$, it can be seen from (20) for a given bandwidth b that as D gradually decreases, the relative position of b and D in the $D - b$ plane successively corresponds to the location of the spacing-dominant, transition, and bandwidth-dominant regions as shown in Fig. 6. When D is large, which corresponds to the spacing-dominant region in the $D - b$ plane, the predicted tracking error decreases linearly with decreasing D . When D is medium, which corresponds to the transition region in the $D - b$ plane, it can be seen from (15) and (20) that the effect of Y on final predicted tracking error is square, while the effect of Γ on final predicted tracking error is approximately linear. Therefore, Y , where the only variable is $\cos(\pi bD/(2\alpha))$, has a major impact on the final tracking error. Considering

the boundary of the transition region $\alpha \leq bD < 3\alpha$, (20) and Fig. 5, it is not difficult to prove that as D decreases in the transition region, the final predicted tracking error decreases first and then increases. Moreover, the minimum of predicted tracking error appears near $bD = 2\alpha$. When D is small, which corresponds to the bandwidth-dominant region in the $D - b$ plane, it can be clearly seen from (15) and (20) that the final predicted tracking error monotonically increases as D decreases. Therefore, to sum up, when $b \geq 3\alpha$, the quasi-optimal subcarrier discriminator spacing D should be set near $2\alpha/b$.

When $b < 3\alpha$, the relative position of b and D in the $D - b$ plane corresponds to the location of the complicated region. It can be seen from the numerical results shown in the following section that, as D decreases in the complicated region for a given bandwidth, the final predicted tracking error is almost constant at first and then gradually increases when D is less than 0.5. Therefore, when D is larger than 0.5 under a given bandwidth in the complicated region, the predicted tracking error is approximately at the minimum value for this bandwidth. Considering that the larger early–late spacing could lead to better dynamic adaptability for GNSS receivers (Kaplan and Hegarty 2005), it should be preferred to choose larger early–late spacing under the similar tracking performance.

Based on the above analysis, in order to ensure the simplicity of the results and the unity of the form, the quasi-optimal early–late subcarrier discriminator spacing D_{opt} under given bandwidth should be set near

$$D_{\text{opt}} = \begin{cases} 1 & b < 2\alpha \\ 2\alpha/b & b \geq 2\alpha \end{cases} \quad (23)$$

where b is the normalized one-sided front-end bandwidth and α is the BOC signal modulation order.

The red dotted line in Fig. 6 shows the location of this conclusion in the $D - b$ plane. Therefore, in order to achieve quasi-global optimal tracking performance for a given bandwidth using DET, the code early–late spacing should be set near to odd multiples of the subcarrier chip period, and the normalized subcarrier early–late spacing D should be set near to $D = 2\alpha/b$ when $b > 2\alpha$ and $D = 1$ when $b < 2\alpha$.

Although, for a given bandwidth, this quasi-optimal discriminator parameter selection rule (23) is obtained by using the closed-form analytical approximation (20) where $\Delta_c = 1 \cdot T_s$, it should be noted that this rule can be directly applied to other cases using the exact expression with Δ_c confined to any other odd multiples of T_s , which will be verified by the numerical results shown in the next section. Therefore, this conclusion provides further guidance to the selection and optimization of receiver parameters while greatly simplifying the work of the receiver designers.

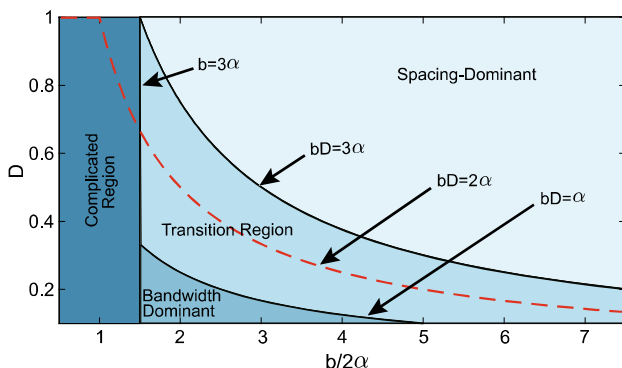


Fig. 6 Region boundaries of closed-form analytical approximation

Numerical results

This section compares numerical results that use the exact expression (9), the closed-form analytical approximation (20), and the infinite bandwidth approximation given in (Borio 2014b, Eq. 32). The results are calculated using a $\text{BOC}_{\sin}(2,1)$ signal, code early–late spacing of $\Delta_c = 1 \cdot T_s$, the coherent integration time of $T = 0.001$ s, and a one-sided equivalent rectangular bandwidth of $B_L = 1$ Hz. It is not difficult to verify that the general conclusions derived from these numerical results can be applied to other $\text{BOC}_{\sin}(\alpha k, k)$ signals and are applicable no matter if Δ_c is any other odd multiple of T_s .

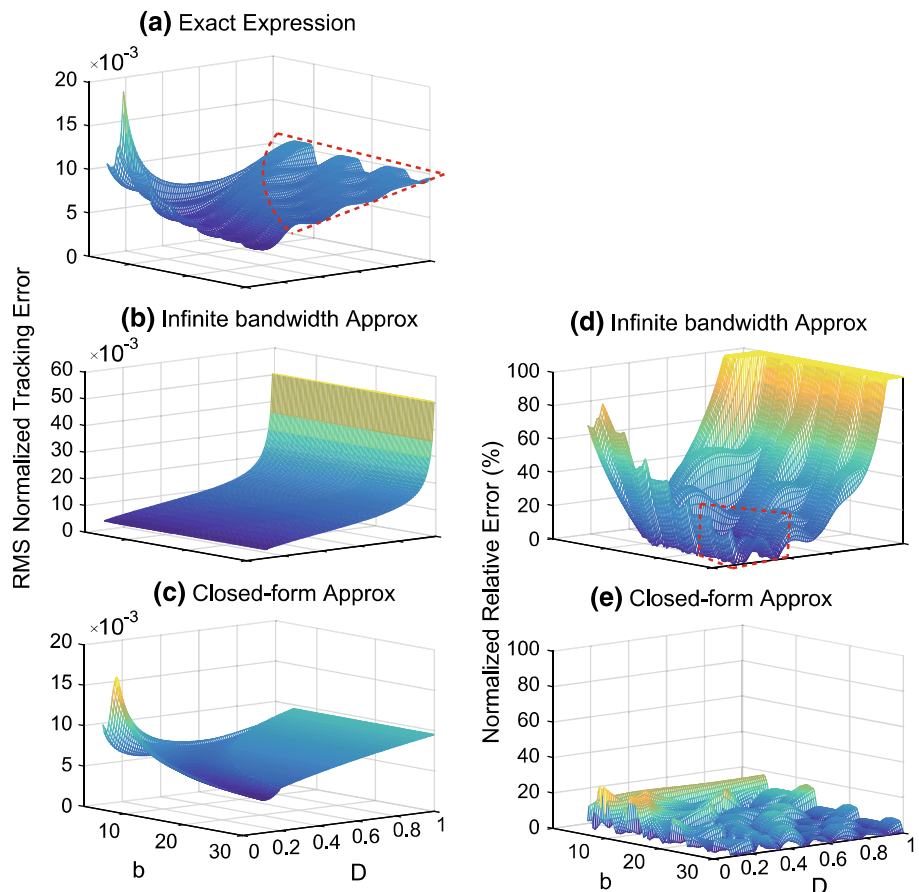
Three-dimensional comparison

The left panels (a)–(c) in Fig. 7 show the normalized tracking error predicted by the exact expression, the infinite bandwidth approximation, and the closed-form analytical approximation, respectively. The right panels (d) and (e) show the absolute value of the normalized relative error between the exact expression and the approximation expressions using the infinite bandwidth approximation as well as the closed-form analytical approximation, respectively. All these results

are obtained over a range of normalized one-sided front-end bandwidths b and early–late subcarrier discriminator spacings D to provide an overall understanding of the influence of these key receiver parameters on final tracking accuracy.

Compared with the left panels (a)–(c), it can be easily seen in the right panels that some main characteristics of the exact expression cannot be found in the infinite bandwidth approximation while they are evident in the closed-form approximation. First, there are four regions of receiver parameter space, shown in Fig. 6, which need to be considered separately. Second, the predicted tracking error increases rather than approaches zero for diminishing subcarrier spacing when D is less than D_{opt} . This is the reason why D_{opt} is chosen as the quasi-optimal early–late subcarrier discriminator spacing. These complicated yet interesting characteristics, shown for the first time, reflect the unique feature of 2-D tracking and need to be adequately considered by the receiver designers to optimize the performance. Of course, in order to allow the closed-form approximation to remain simple while preserving the main characteristics, some concessions are made, such as the oscillatory characteristic of the spacing-dominant region enclosed by the red dotted line in panel (a). This concession is a small price to pay for increased computational efficiency.

Fig. 7 Predicted tracking error evaluated at $C/N_0 = 35$ dB Hz using **a** the exact expression, **b** the infinite bandwidth approximation, and **c** the closed-form analytical approximation; Absolute value of normalized relative error between the exact expression and **d** the infinite bandwidth approximation, **e** the closed-form analytical approximation



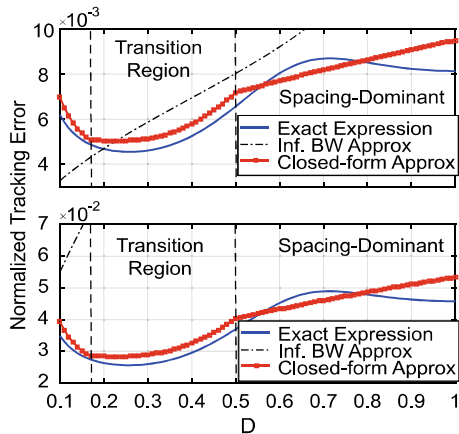


Fig. 8 Predicted tracking error for normalized front-end bandwidth of 12 and C/N_0 of (top) 35 dB Hz and (bottom) 20 dB Hz

Compared with the right panels (d) and (e), it can be confirmed that the closed-form approximation performs better than the infinite bandwidth approximation with respect to the exact expression. Although the relative error of the area enclosed by the red dotted line in panel (d) is small, it is large in other regions especially for small b or for large D . Meanwhile, the relative error is consistently small over the entire range of parameters in panel (e), and in some regions it is even $< 10\%$. Even in the complicated region, the relative error does not exceed 26%. Therefore, the closed-form approximation without numerical integration can be used instead of the exact expression to quickly predict the tracking error.

Profile comparison

While the surfaces shown in Fig. 7 qualitatively indicate the behavior of these expressions, more quantitative results are obtained by considering slices of these surfaces.

Performance comparison of different C/N_0

Figure 8 shows the predicted tracking error for a normalized front-end bandwidth of $b = 12$ and different C/N_0 , one being 35 dB Hz in the top panel and another being 20 dB Hz in the bottom panel. Contrasting the top and bottom panels, it can be easily seen that the closed-form approximation always tracks the exact expression very well under different values of C/N_0 , while the infinite bandwidth approximation performs well only in a high C/N_0 case. Additionally, both the exact expression and the closed-form approximation show that when D is less than D_{opt} , the predicted tracking error will increase for diminishing D , while the infinite bandwidth approximation shows the tracking error approaches zero under the same condition. Considering the infinite

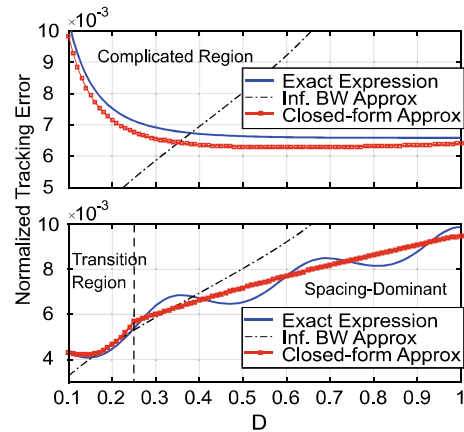


Fig. 9 Predicted tracking error for C/N_0 of 35 dB Hz and normalized front-end bandwidth of (top) 3 and (bottom) 24

bandwidth approximation is only applicable in a high C/N_0 case, the remaining results are evaluated at C/N_0 of 35 dB Hz.

Performance comparison of different front-end bandwidth b

The following analysis will select three representative cases for performance comparison of different front-end bandwidths, which are $b = 3$, corresponding to a narrow bandwidth, $b = 12$, corresponding to a moderate bandwidth, and $b = 24$, corresponding to a wide bandwidth.

The results of $b = 12$ are shown in the top panel in Fig. 8. Figure 9 shows the predicted tracking error of $b = 3$ in the top panel and $b = 24$ in the bottom panel. Comparing these three panels, both the exact expression and the closed-form approximation show that when D is close to D_{opt} , there will be a reversal in the predicted tracking error for diminishing D while the infinite bandwidth approximation shows the tracking error decreases monotonically to zero. In addition, it can be easily seen that the closed-form approximation always matches the exact expression very well for different bandwidths while the infinite bandwidth approximation performs well only in the high bandwidth case. More importantly, the top panel in Fig. 9 shows the tracking error predicted by the exact expression, and the closed-form approximation with a narrow bandwidth is almost constant at first and then gradually increases for diminishing D , while the infinite bandwidth approximation shows the tracking error decreases monotonically to zero. This phenomenon implies that the coupling relation between dimensions and the effects of band-limiting are so important that they cannot be ignored especially when the bandwidth is narrow.

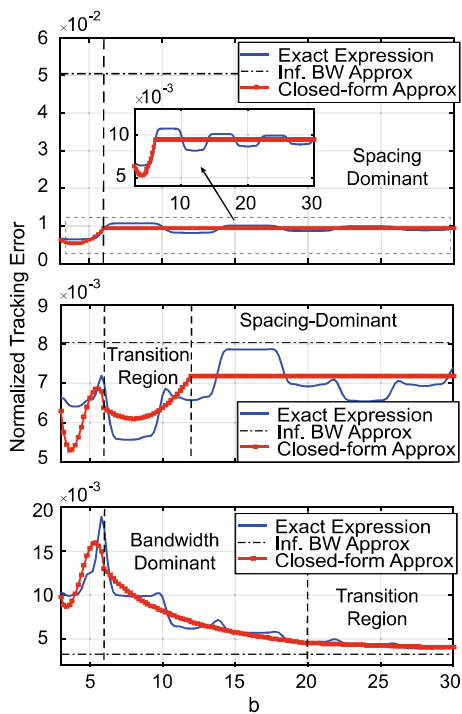


Fig. 10 Predicted tracking error for C/N_0 of 35 dB Hz and normalized subcarrier discriminator spacing of (top) 1, (middle) 0.5, and (bottom) 0.1

Performance comparison of different early–late spacing D

The following analysis will select three representative cases for performance comparison of different early–late spacing, which are $D = 1$, corresponding to a wide spacing, $D = 0.5$, corresponding to a moderate spacing, and $D = 0.1$, corresponding to a narrow spacing.

The top, middle, and bottom panels in Fig. 10 show the predicted tracking error of $D = 1$, $D = 0.5$ and $D = 0.1$, respectively. Comparing these three panels, the following characteristics can be seen. First, both the exact expression and the closed-form approximation show that the front-end bandwidth does have an influence on the final tracking error, while the infinite bandwidth approximation shows the tracking error has no dependence on the front-end bandwidth. Second, it can be easily seen that the closed-form approximation always tracks the exact expression very well under different early–late spacing, while the infinite bandwidth approximation overestimates the error for wider spacing and underestimates the error for narrow spacing. Third, it can be seen from both the exact expression and the closed-form approximation that increased bandwidth can lead to significant improvements of tracking performance only in the bandwidth-dominant region while it cannot do so in the other regions. Fourth, when $b < 3\alpha$, corresponding to the complicated region, predicted tracking errors using the exact

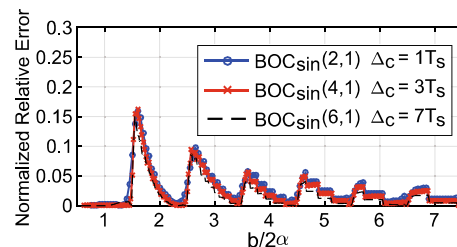


Fig. 11 Absolute value of the normalized relative error between tracking error predicted with quasi-optimal discriminator parameter selection rule and tracking error minima predicted by the exact expression for $\text{BOC}_{\sin}(ak, k)$ signal and $\Delta_c = iT_s$, $i = 1, 3, 7$

expression and the closed-form approximation become very complex due to the effects of band-limiting and the coupling relation between dimensions. This is why the parameter set to $b < 3\alpha$ is called the complicated region.

Optimal receiver parameters selection

The oscillatory behavior of the exact expression for predicted tracking error can be observed in Figs. 7, 8, 9, and 10. It can be seen from these figures that the tracking performance is very sensitive to the variations of bandwidths and early–late spacing. Over relatively small ranges of front-end bandwidths and early–late spacing, the RMS tracking error oscillates over a peak-to-peak range of about 25 percent. Therefore, choosing an appropriately matched bandwidth and spacing can significantly lower the tracking error.

It is shown in Figs. 8, 9, and 10 that there are local minima in the predicted tracking error for $bD = 2\alpha, 6\alpha, 10\alpha, \dots$. Conversely, there are local maxima in the predicted tracking error for $bD = 4\alpha, 8\alpha, 12\alpha, \dots$. Consequently, there may be advantages in selecting paired values of front-end bandwidth and discriminator spacing that avoid these local maxima and seek the local minima in the acquisition and tracking process of receivers using DET for BOC signals.

Moreover, it is shown in Figs. 8 and 9 that the minimum tracking error for a given bandwidth occurs near $bD = 2\alpha$ for $b > 2\alpha$ and $D = 1$ for $b < 2\alpha$, which verifies the correctness of the quasi-optimal discriminator parameters selection rule for a given bandwidth (23).

Although the above simulations are based on the $\text{BOC}_{\sin}(2,1)$ signal and early–late code discriminator spacing of $\Delta_c = 1 \cdot T_s$, the following simulation results verify that the quasi-optimal discriminator parameters selection rule under given bandwidth (23) can be directly applied to other $\text{BOC}_{\sin}(ak, k)$ signals and are applicable no matter if Δ_c is any other odd multiple of T_s .

Figure 11 shows absolute value of a normalized relative error between the tracking error predicted with the quasi-optimal discriminator parameter selection rule (23) and

the minimum tracking error predicted by the exact expression for a $\text{BOC}_{\sin}(\alpha k, k)$ signal for a given bandwidth when $\Delta_c = iT_s$, $i = 1, 3, 7$. When b is small, which corresponds to the complicated region in the receiver parameter space, the tracking accuracy predicted using the quasi-optimal parameter selection rule (23) is very accurate as compared to the theoretical optimal. As b increases, the relative error becomes gradually smaller indicating that the quasi-optimal discriminator parameter selection rule (23) is more accurate for wider bandwidths. Within the entire range of the bandwidths, the maximum relative error is only about 16%. Therefore, in order to achieve quasi-global optimal tracking performance under given bandwidth using DET for $\text{BOC}_{\sin}(\alpha k, k)$ signals, the code early–late spacing should be set near to odd multiples of subcarrier chip period, and the normalized early–late subcarrier discriminator spacing D should be set near to $D_{opt} = 2\alpha/b$ when $b > 2\alpha$ and $D_{opt} = 1$ when $b < 2\alpha$. This conclusion can provide strong guidance for the selection and optimization of receiver parameters and thus greatly simplify the work of the receiver designers while improving the tracking performance.

Conclusions and future work

We have presented the derivation and numerical evaluation of tracking performance analysis and optimal discriminator parameters selection in white noise for limited front-end bandwidths using DET for BOC signals processing. The work and contribution of our discussion mainly include three aspects.

First, the exact expression for tracking performance prediction is provided to describe how well DET could perform for given conditions that are of concerned to receiver designers, e.g., receiver front-end bandwidth, early–late code discriminator spacing and early–late subcarrier discriminator spacing. It can be seen from the exact expression that the selection of code early–late spacing significantly affects the final tracking accuracy, and in order to achieve better tracking performance, the code early–late spacing should be set near to odd multiples of the subcarrier chip period rather than even multiples.

Second, the closed-form analytical approximation with code early–late spacing confined to odd multiples of subcarrier chip period is presented since the evaluation of the exact expression requires numerical integration. The closed-form analytical approximation shows that there are four regions of receiver parameter space that need to be considered separately. These regions are defined in terms of the normalized front-end bandwidth b , which is the ratio of the one-sided front-end bandwidth to the spreading code rate, the normalized early–late subcarrier discriminator spacing D , which

is the two-sided spacing of the subcarrier discriminator expressed as a fraction of the subcarrier chip period, and the BOC signal modulation order α .

The region defined by $bD \geq 3\alpha$ is referred to as spacing-dominant, since the predicted tracking error depends primarily on the subcarrier early–late spacing but not the front-end bandwidth. The region defined by $bD < \alpha$ and $b \geq 3\alpha$ is referred to as bandwidth-dominant since the early–late subcarrier spacing is restricted to a limited range and the predicted tracking error is mainly determined by the front-end bandwidth. The condition $\alpha \leq bD < 3\alpha$ and $b \geq 3\alpha$ indicates a transition region between the two distinct dominant cases. The region defined by $b < 3\alpha$ is referred to as the complicated region, since the predicted tracking error is complicated due to the effects of band-limiting and the coupling relation between the code delay and subcarrier delay dimension.

Third, a quasi-optimal discriminator parameters selection rule for a given bandwidth is also provided for further receiver design guidance. In order to achieve quasi-global optimal tracking performance for a given bandwidth using DET, the code early–late spacing should be set near to an odd multiple of the subcarrier chip period, and the normalized subcarrier early–late spacing D should be set near to $D = 2\alpha/b$ when $b > 2\alpha$ and $D = 1$ when $b < 2\alpha$.

With the increasing interest in 2-D tracking techniques, theoretical analysis of tracking performance using DET for BOC signals processing is likely to take on continuing importance in receiver designs. Therefore, the tracking performance prediction using the exact expression and the closed-form analytical approximation presented should both be employed to provide further guidance into receiver designs. Additionally, the quasi-optimal discriminator parameters a selection rule for a given bandwidth could be used to simplify the work of the receiver designers while improving the tracking performance. For instance, these results can be directly applied to the unmatched tracking mode of multiplexed BOC (MBOC), which means when BOC(1,1) is used to track the composite BOC (CBOC) and time-multiplexed BOC (TMBOC)-modulated signals, and the results can provide further guidance for the parameter selection and optimization of the receiver design. For future research, the 2-D tracking theory and performance analysis of Alternative BOC (AltBOC) signals can be carried out based on results presented herein. Furthermore, multipath performance analysis and multipath mitigation techniques with 2-D tracking loops are recommended for future research.

Acknowledgements This work is supported by National Natural Science Foundation of China (NSFC), under Grant 61771272.

Appendix derivation of closed-form analytical approximation expression

Considering the $\text{BOC}_{\sin}(\alpha k, k)$ signal, assume the normalized one-sided front-end bandwidth is wide enough to contain two main lobes of the $\text{BOC}_{\sin}(\alpha k, k)$ signal spectrum, i.e., $b \geq \alpha + 1$. Substituting $\Delta_c = 1 \cdot T_s$ into (11) and (12), one can obtain the normalized slope matrix

$$\begin{aligned}\kappa_{cc} &= \frac{1}{\alpha\pi} \left(2\text{Si}\left(\frac{b}{2\alpha}\pi\right) + \text{Si}\left((4\alpha-1)\frac{b}{2\alpha}\pi\right) - \text{Si}\left((4\alpha+1)\frac{b}{2\alpha}\pi\right) \right) \\ \kappa_{cs} &= \kappa_{sc} \\ &= -\frac{4}{\alpha\pi} \left(\sum_{m=1}^{2\alpha-1} (-1)^{m+1} \text{Si}\left(m\frac{b}{\alpha}\pi\right) - \frac{1}{2} \cdot \text{Si}(2b\pi) \right) \\ \kappa_{ss} &= \frac{2}{\alpha\pi} \left[\sum_{m=1}^{2\alpha} \left[(-1)^{m+1} (2m-1) \text{Si}\left(\frac{b}{2\alpha}\pi(D-(4\alpha+2-2m))\right) \right. \right. \\ &\quad \left. \left. + (-1)^m (2m-1) \text{Si}\left(\frac{b}{2\alpha}\pi(D+(4\alpha-2m))\right) \right] \right]\end{aligned}\quad (24)$$

Using the approximation relation (18) then (24) can be further approximately simplified as (21). So (16) can be simplified as

$$Y \approx \begin{cases} \left(\frac{\alpha}{4\alpha-1}\right)^2 & bD \geq 3\alpha \\ \left(\frac{\alpha\pi}{2(4\alpha-1)(-0.28\cos(\frac{bD}{2\alpha}\pi)+\frac{\pi}{2})}\right)^2 & b \geq 3\alpha, \alpha < bD < 3\alpha \\ \left(\frac{a^2}{(4\alpha-1)bD}\right)^2 & b \geq 3\alpha, bD \leq \alpha \\ \frac{\tilde{\kappa}_{sc}^2 + \kappa_{cc}^2 - \tilde{\kappa}_{sc}\tilde{\kappa}_{cc}}{3 \cdot (\tilde{\kappa}_{sc}\tilde{\kappa}_{ss} - \tilde{\kappa}_{cs}\tilde{\kappa}_{sc})^2} & b < 3\alpha \end{cases}\quad (25)$$

Similarly, for (17) there is

$$\Gamma = \frac{1}{b\pi^2} \left\{ \begin{array}{l} -(8\alpha+2) + 8F\left(\frac{b}{2\alpha}\pi(D-1)\right) \\ -4F\left(\frac{b}{2\alpha}\pi(D-(4\alpha+1))\right) - 4F\left(\frac{b}{2\alpha}\pi(D-(4\alpha-1))\right) \\ + \sum_{m=1}^{4\alpha-1} c_m \cdot F\left(\frac{b}{\alpha}\pi(D-(2\alpha-m+1))\right) \\ + \sum_{m=1}^{2\alpha+1} a_m \cdot F\left(m\frac{b}{\alpha}\pi\right) \end{array} \right\}\quad (26)$$

where a_m and c_m are integer coefficient, which can be eliminated using the approximation relation (19). Substituting (19) into (26), after simplification one can obtain

$$\Gamma \approx \begin{cases} \left(4 - \frac{2}{\alpha}\right)D + \frac{1}{\alpha} & b \geq 3\alpha, bD \geq \alpha \\ \frac{2(2\alpha-1)}{\alpha^2}bD^2 + \frac{1}{\alpha} & b \geq 3\alpha, bD < \alpha \\ \zeta & b < 3\alpha \end{cases}\quad (27)$$

Substituting (25) and (27) into (15), we obtain the final closed-form analytical approximation expression (20).

References

- Anantharamu PB, Borio D, Lachapelle G (2009) Pre-filtering, side-peak rejection and mapping: several solutions for unambiguous BOC Tracking. In: Proceedings ION GNSS 2009, Savannah, Georgia, USA, 22–25 September, pp 3142–3155
- Betz JW (1999) The Offset carrier modulation for GPS modernization. In: Proceedings ION NTM 1999, San Diego, California, USA, 25–27 January, pp 639–648
- Betz JW (2001) Binary offset carrier modulations for radionavigation. *Navig J Inst Navig* 48(4):227–246
- Betz JW, Kolodziejczyk KR (2000) Extended theory of early-late code tracking for a bandlimited GPS receiver. *Navig J Inst Navig* 47(3):211–226
- Betz JW, Kolodziejczyk KR (2009a) Generalized theory of code tracking with an early-late discriminator part I: lower bound and coherent processing. *IEEE Trans Aerosp Electron Syst* 45(4):1538–1550
- Betz JW, Kolodziejczyk KR (2009b) Generalized theory of code tracking with an early-late discriminator part II: noncoherent processing and numerical results. *IEEE Trans Aerosp Electron Syst* 45(4):1551–1564
- Borio D (2014a) Double phase estimator: new results. Satellite navigation technologies and European workshop on GNSS signals and signal processing (NAVITEC) 2014 7th ESA workshop on, Noordwijk, Netherlands, 3–5 December, pp 1–6
- Borio D (2014b) Double phase estimator: new unambiguous binary offset carrier tracking algorithm. *IET Radar Sonar Navig* 8(7):729–741
- Fine P, Wilson W (1999) Tracking algorithm for GPS offset carrier signals. In: Proceedings ION NTM 1999, San Diego, California, USA, 25–27 January, pp 671–676
- Hodgart MS, Simons E (2012) Improvements and additions to the double estimation technique. Satellite navigation technologies and European workshop on GNSS signals and signal processing (NAVITEC) 2012 6th ESA workshop on, Noordwijk, Netherlands, 5–7 December, pp 1–7
- Hodgart MS, Blunt P, Unwin M (2007) The optimal dual estimate solution for robust tracking of binary offset carrier (BOC) modulation. In: Proceedings ION GNSS 2007, Fort Worth, Texas, USA, 25–28 September, pp 1017–1027
- Julien O, Macabiau C, Bertrand E (2010) Analysis of Galileo E1 OS unbiased BOC/CBOC tracking techniques for mass market applications. Satellite navigation technologies and European workshop on GNSS signals and signal processing (NAVITEC) 2010 5th ESA workshop on, Noordwijk, Netherlands, 8–10 December, pp 1–8
- Kao TL, Juang JC (2012) Weighted discriminators for GNSS BOC signal tracking. *GPS Solut* 16(3):339–351
- Kaplan ED, Hegarty C (2005) Understanding GPS: principles and applications. Artech House, Norwood
- Mongredien C, Rügamer A, Overbeck M, Rohmer G, Berglez P, Wasle E (2011) Opportunities and challenges for multi-constellation, multi-frequency automotive GNSS receivers. In: Heuberger A (ed) Microelectronic systems. Springer, Berlin, pp 159–172
- Rebeyrol E, Julien O, Macabiau C, Ries L, Delatour A, Lestarquit L (2007) Galileo civil signal modulations. *GPS Solut* 11(3):159–171
- Ruegamer A et al (2011) A Bavarian Initiative towards a Robust Galileo PRS Receiver. In: Proceedings ION GNSS 2011, Portland, Oregon, USA, September 20–23, pp 3668–3678

Yao Z, Cui X, Lu M, Feng Z (2010) Pseudo-correlation-function-based unambiguous tracking technique for Sine-BOC signals. *IEEE Trans Aerosp Electron Syst* 46(4):1782–1796

Yao Z, Gao Y, Gao Y, Lu M (2017) Generalized theory of BOC signal unambiguous tracking with two-dimensional loops. *IEEE Trans Aerosp Electron Syst* 53(6):3056–3069



Yang Gao received the B.Eng. degree in electronic information science and technology in 2013 from Tsinghua University, Beijing, China, where he is currently working toward the Ph.D. degree in information and communication engineering. His current research focuses on new-generation GNSS signal processing and real-time GNSS software receiver.



and receiver development.

Mingquan Lu is a Professor with the Department of Electronic Engineering, Tsinghua University, Beijing, China. He received the M.E. and Ph.D. degrees in electrical engineering from the University of Electronic Science and Technology of China, Chengdu, China. He directs the Positioning, Navigation and Timing (PNT) Research Center, which develops GNSS and other PNT technologies. His current research interests include GNSS system modeling and simulation, signal design and processing,



Zheng Yao is an Associate Professor with the Department of Electronic Engineering, Tsinghua University, Beijing, China. He received the B.E. degree in electronics information engineering and the Ph.D. degrees (with the highest honors) in information and communication engineering from Tsinghua University, Beijing, China, in 2005 and 2010, respectively. His current research mainly targets next-generation satellite navigation signals design, software-defined receiver, new location technologies, and personal and vehicular positioning in challenging environments.